Functional Analysis of Battery Management Systems using Multi-Cell HIL Simulator

Barreras, Jorge Varela; Swierczynski, Maciej Jozef; Schaltz, Erik; Andreasen, Søren Juhl; Fleischer, Christian; Sauer, Dirk Uwe; Christensen, Andreas Elkjær

Published in:
Proceedings of the 2015 Tenth International Conference on Ecological Vehicles and Renewable Energies (EVER)

DOI (link to publication from Publisher):
10.1109/EVER.2015.7112984

Publication date:
2015

Document Version
Early version, also known as pre-print

2015 Tenth International Conference on Ecological Vehicles and Renewable Energies (EVER)

Functional Analysis of Battery Management Systems using Multi-Cell HIL Simulator

Jorge Varela Barreras
Maciej Swierczynski
Erik Schaltz
Søren Juhl Andreasen
Aalborg University, Denmark
jvb@et.aau.dk

Christian Fleischer
Dirk Uwe Sauer
ISEA - RWTH Aachen University
Germany
Christian.Fleischer@isea.rwth-aachen.de

Andreas Elkjær Christensen
Lithium Balance A/S, Denmark
DTU Energy,
Tech. University of Denmark
andreas@lithiumbalance.com

***Abstract*—Developers and manufacturers of Battery Management Systems (BMSs) require extensive testing of controller HW and SW, such as analog front-end (AFE) and performance of generated control code. In comparison with tests conducted on real batteries, tests conducted on hardware-in-the-loop (HIL) simulator may be more cost ant time effective, easier to reproduce and safer beyond the normal range of operation, especially at early stages in the development process or during fault simulation. In this paper a li-ion battery (LIB) electro-thermal multi-cell model coupled with an aging model is designed, characterized and validated based on experimental data, converted to C code and emulated in real-time with a dSpace HIL simulator. The BMS to be tested interacts with the emulated battery pack as if it was managing a real battery pack. BMS functions such as protection, measuring of current, voltage and temperature or balancing are tested on real-time experiments.**

***Keywords*—battery management system; hardware-in-the-loop; lithium ion.**

I. Introduction

A well-known limitation of LIBs is the need of reliable electronic protection, i.e. a BMS, to avoid electric or thermal abuse. The reason for this is to minimize battery degradation and to prevent thermal instability, conditions that can lead certain chemistries to a thermal runaway.

Moreover, in order to maximize battery capacity, active or passive balancing circuits are implemented in BMSs. Without balancing, if multiple cells are connected in series, the weakest cell constraints the entire pack performance. Local operational differences and uncertainties at the material level are related to these cell-to-cell variations, which lead to further differences in the cell-to-cell performance over time.

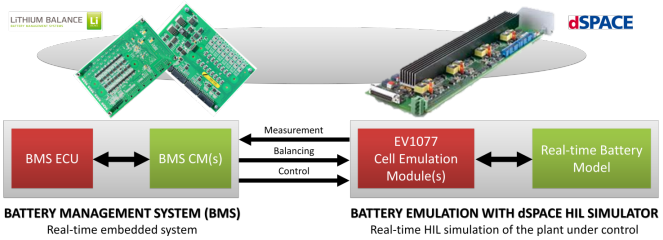

Fig. 1: Concept of high-precision cell voltage emulation.

In this paper a LIB electro-thermal multi-cell equivalent circuit model (ECM) coupled with an aging model is designed, characterized and validated based on experimental data, converted to C code and emulated in real-time with a dSpace HIL simulator (see Fig.1 and Fig.2). The HIL simulator is able to provide signals for testing a wide variety of BMS functions, such as cell protection; safety validation; measuring of current, voltage and temperature; balancing of cells; analysis and parameter prediction; logging, telemetry and external communications.

The paper is organized as follows. In Section II the concept of battery emulation is reviewed based on literature. In Section III the proposed electro-thermal LIB pack model is presented and parameterized based on experimental data from large format NMC Li-ion pouch cells. In Section IV the commercial BMS under test is briefly described. In Section V experimental results of the interaction of the BMS with the emulated battery pack are provided. Finally, Section VI gives the conclusions.

II. Critical Review of Battery Emulation

Nowadays HIL simulators are widely employed to prototype, design and test complex real-time systems in many applications due to a combination of safety, feasibility, time and cost effectiveness factors. In the next

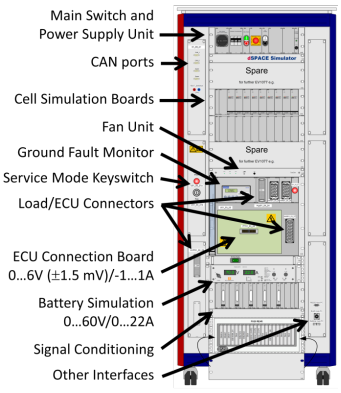

(a) Overview of dSpace HIL Simulator

(b) Picture of the Lithium Balance sBMS under test, connected to the dSpace HIL Simulator.

Fig. 2: Setup of Hardware-in-the-Loop test bench.

section, the HIL simulation approaches in relation with LIBs presented in scientific and technical literatures are reviewed with a special focus on automotive applications.

HIL simulation uses some virtual or emulated components and some physical components. If a real LIB system is used, the method is so called battery-in-the-loop (BIL) or battery-hardware-in-the-loop (BHIL). BIL simulation is proposed in automotive applications for the purposes of battery evaluation [1], BMS validation [2], verification of battery models [3] or assessment of power or energy management strategies [4]-[6], considering a complete virtual vehicle [1]-[4] or in combination with other real components [5],[6].

HIL simulation methods with virtual LIBs, pack-based (or aggregated) approaches [7]-[22] are more frequent in literature than cell-based (or multi-cell) approaches [23]-[32]. In general, in order to control the charging/discharging process, any BMS for a series or series-parallel connected battery pack should at least monitor the pack voltage, the pack current, the single cell voltages and the temperatures at cell or pack level. Moreover, cell balancing is required to avoid severe state of charge unbalances over time due to cell-to-cell differences [33]. Hence, it is easy to understand that, for purposes of complete BMS validation, cell-based HIL simulation is preferred over pack-based.

HIL simulation using virtual LIB pack-based methods is proposed in stationary [20]-[22] and automotive applications [7]-[19], the latter with the goal of electric powertrain evaluation [7]-[11], BMS validation [12],[13], vehicle controller unit testing [14], assessment of power or energy management strategies [15],[16] or verification of the feasibility of the HIL concept [17],[18]. On the other hand, HIL simulation using virtual LIB cell-based methods is proposed either for addressing BMS validation [23]-[31] or only testing balancing circuits [32].

If there is high power flow between real components and the HIL simulator, the technique is called power-hardware-in-the-loop (PHIL) [7]-[11], [15], [16], [18]-[20]. This a common feature of pack-based HIL simulators used for electric powertrain evaluation [7]-[11]. PHIL simulation is also applied in [19] to lead-acid technology, where a portable system using virtual 12V SLI battery is presented and tested during motor cranking in a car.

In contrast, the usual case in HIL simulation only involves low level of power, voltage and current related with analog and digital I/O signals or communication networks, e.g. CAN bus [1]-[6], [12]-[14], [17], [21]-[32]. In general, this is the case of all the cell-based HIL simulation approaches found in literature [23]-[32]. In some cases a strictly communication based approach is proposed [14], [21]-[25], [29], which means that BMS functions such as measuring or balancing cannot be tested, either at cell or pack level.

Regarding balancing, an isolated power interface for each cell in series (or group of cells in parallel in case of a series-parallel connected pack) is desired to exchange bi-directional power flow between virtual cells and real electric circuits. But such interface is only presented in cell-based simulators described in [30]-[32]. Results are shown, respectively, for only 1, 4 or 6 cells in series, and current levels at 200 mA, 1.45 A, or 5 A. Moreover, it should be noted that the setup presented in [32] is only targeted for testing balancing circuits, and not for testing any other BMS functions.

With regards to the temperature emulation, it is claimed in several references, but the thermal model is either not described [12], [13], [17], [23], [26] or the temperature is artificially introduced [24]. In fact, a thermal model is only presented in [18]. However, a pack-based approach is followed and the lumped equivalent circuit model described is parameterized without experimental data. Moreover, the self-made HIL simulator setup presented can only run discharging profiles.

The most common approach for battery modelling methods are electrical models based on ECMs, e.g. impedance-based modeling (abstract approach) [3], [7]-[13], [16], [18]-[21], [25], [26], [30]-[32]. Other approaches are proposed rarely in the literature. ECMs can provide information about the macroscopic quantities that are monitored by a BMS, i.e. current, voltage and temperature (if a thermal model is included), offering a better trade-off between complexity and accuracy than other mathematical or physic-chemical approaches, like

the ones proposed in [7] and [15]. In [7] an extended modified Shepherd model (abstract approach) is proposed, and in [15] a Dual-foil based-model (physic-chemical approach).

However, ECMs do not allow extrapolation from one material or cell designs to another one. Therefore, for a universal BMS validation, a library of battery models for different cell sizes, formats, chemistries and manufacturers are desired. Such a library is not presented in the reviewed literature [1]-[32].

Moreover, the accuracy of the ECM lays on the circuit topology and the component dependencies on state-of-charge (SOC), state-of-health (SOC), current or temperature. The common approach is to use non-linear dynamic ECMs with two RC elements. This circuit topology may account for most important dynamic effects. However, simple or no dependencies are usually considered in literature. For example, only SOC dependencies in open circuit voltage are considered in [8], [10], [20], [21], [25], [31] and the dependencies are not considered or are not well defined in [9], [11], [12], [17], [18], [23], [24].

It should be noted that even if a non-linear dynamic ECM with two RC elements is used, the model may not reproduce accurately realistic battery profiles if only a few or non-dependencies are considered in the circuit components.

Furthermore, in order to account for cell-to-cell differences or emulating different testing scenarios, an aging model may be coupled to the electrical model. This approach is not followed in the reviewed literature [1]-[32]. It should be noted that, for purposes of general functional analysis of a BMS, simpler battery models may be used. However, more accurate models may be implemented with the aim of ensuring that complex functionalities of a BMS, such as diagnostic algorithms for State-of-Charge (SOC), State-of-Function (SOF) or State-of-Health (SOH) estimation, can be analyzed and validated using HIL simulation.

III. Electro-thermal LIB pack model

In this section the LIB electro-thermal multi-cell ECM model coupled with an aging model is designed and characterized for a commercial 40 Ah high-energy Kokam SLPB100216216H pouch cell. The ECM model consists of an inductance, an ohmic resistor and two ZARC elements in series. Experimental pulse power characterization, capacity check, electrochemical impedance spectroscopy (EIS) and anisotropic thermal diffusivity measurement techniques are used for parameter estimation, taking into account aging, temperature and SOC dependencies.

Results are presented for a Kokam cell for illustrative purposes, but a full library has been developed including battery cells with different formats (cylindrical, pouch, prismatic), capacities (2Ah, 53Ah, 100Ah) and chemistries (NMC, LTO, LFP), including manufacturers such as Sanyo, Panasonic and SkyEnergy.

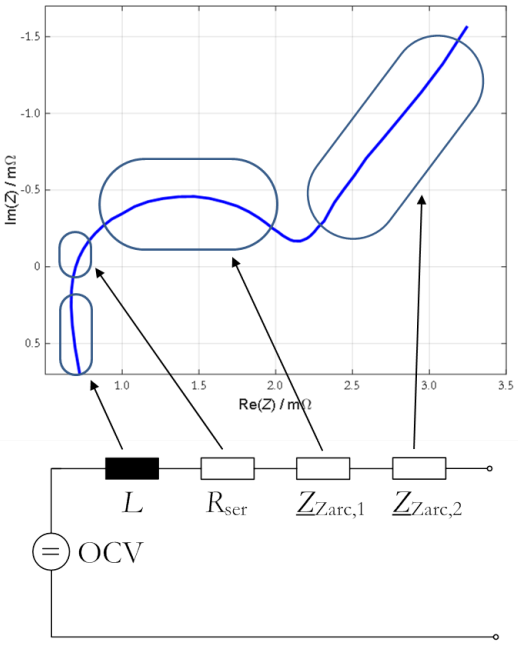

Fig. 3: Mapping of processes from the impedance spectra to equivalent circuit model.

A. Impedance spectrum analysis

In Fig. 4, EIS measurements conducted on the Kokam 40 Ah NMC-cathode cell are presented in a Nyquist plot. At high frequencies (> 0.8 kHz) the cell shows inductive behavior caused by inductive reactance of metallic elements in the cell and wires. This is modeled as an inductor in series in the ECM. At a frequency of 375 Hz pure resistive behavior is observed, related with the sum of the ohmic resistances of current collectors, active material, electrolyte and separator. This effect is modeled as a resistor in the ECM. At lower frequencies, one depressed semi-circle is observed in the spectrum. This is associated to a SEI effect superimposed with the double layer capacity and the charge-transfer resistance at the electrodes. All these effects can be modeled by using a ZARC element in the ECM. At frequencies below 0.375 Hz a linear slope with an angle of $45°$ is observed. This is associated with the diffusion process and can be also approximated by another ZARC element.

A ZARC element is made up of a resistor in parallel

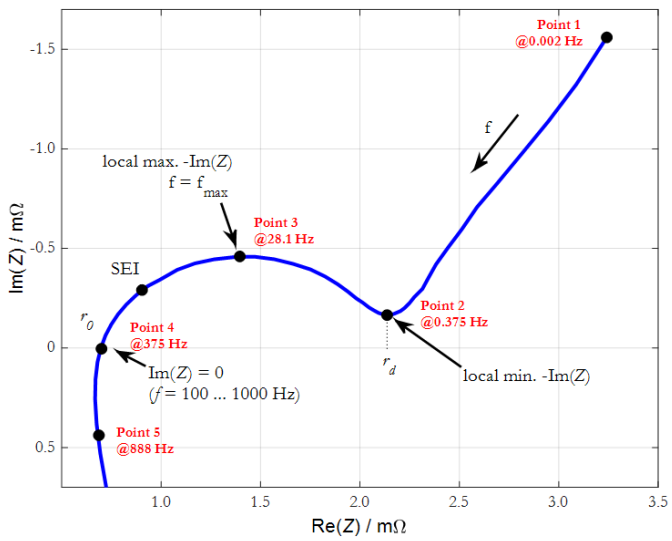

Fig. 4: Nyquist plot of the complex impedance of a Kokam 40 Ah NMC-cathode cell.

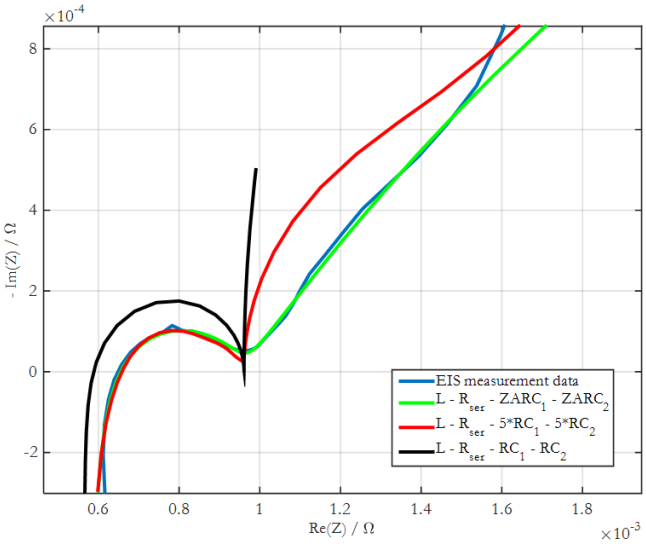

Fig. 6: Comparison of different model approximations.

with a constant-phase-element (CPE):

$$\omega_0 = \left(\frac{1}{A \cdot R}\right)^{\frac{1}{\xi}} \Longleftrightarrow \underline{Z} = A \cdot (j\omega)^{-\xi} \quad (1)$$

$$\omega_{0,\text{ZARC}} = \omega_{0,\text{RC}} = \frac{1}{C_{\text{RC}} \cdot R} \quad (2)$$

$$\Longleftrightarrow C_{\text{RC}} = \frac{1}{\omega_{0,\text{RC}} \cdot R} \quad (3)$$

A CPE consists of a generalized capacity and depression factor. If the depression factor is equal to 1, the ZARC element corresponds to a simple RC element. If it is equal to 0 it just represents a resistor in series.

B. Approximation of ZARC elements

ZARC elements are able to accurately reproduce the impedance spectra of LIBs, but it is impossible to transfer without approximations their parameters from the frequency domain into the time domain. A common method to approximate ZARC elements is using a variable number of RC-elements (Fig. 5). Each of the individual RC elements represents a semicircle in the Nyquist plot. To represent the ZARC exactly, infinite RC elements are needed. Nevertheless, taking into account the computational cost vs. accuracy, a few RC elements are sufficient for a good approximation.

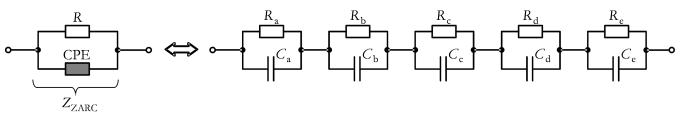

Fig. 5: Approximation of ZARC element through series connection of RC elements [34].

As observed in Fig. 6, the error for 5 RC elements in comparison to the approximation with only 1 RC element is reduced to a satisfactory result. The overall approximation equation is derived as following [34]:

$$\underline{Z}_{2ZARC}(j\omega) = R_{ser} + \frac{R_1}{1 + (j\omega)^{-\xi} \cdot R_1 \cdot C_1} + \frac{R_2}{1 + (j\omega)^{-\xi} \cdot R_2 \cdot C_2} \quad (4)$$

C. ECM parameter identification

Some parameters of the ECM can be directly derived from the impedance spectrum. For example, the series resistance at high frequencies can be estimated from the intersection of the spectrum with the real part axis. Other parameters, like the inductor in series, can be neglected in some cases [35]. For example, if electric vehicle applications are simulated, due to their characteristic slow dynamics. Moreover, it does not make sense to simulate phenomena that cannot be measured due to limited sampling rate of the BMS or the HIL simulator.

An in-house tool based on Matlab Easyfit function is applied to fit the experimental EIS data in order to parameterize the ECM. The Nelder-Mead simplex search algorithm is used, which allows an accurate and precise emulation of the impedance spectra based on the modeling function. This function is crucial, because it defines the quality and robustness of the parameter identification process. It should be noted that it is always useful to define starting parameters derived directly from the impedance spectrum [36].

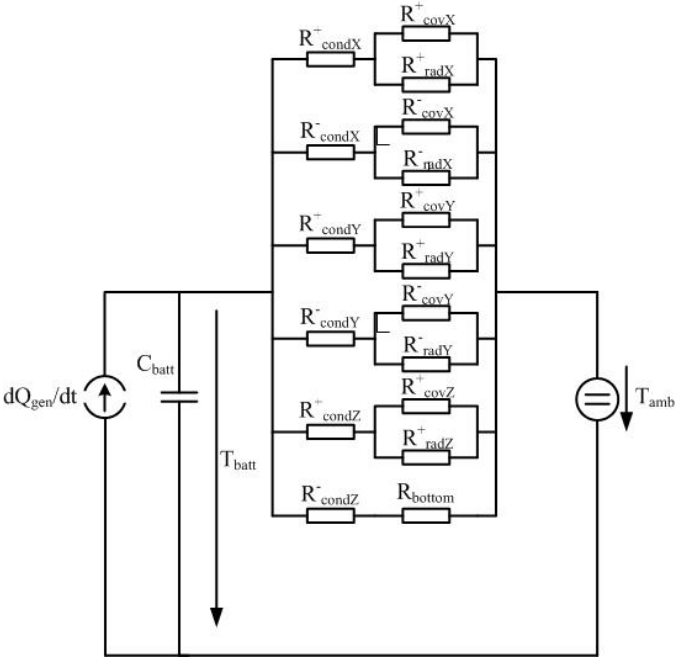

Fig. 7: Employed equivalent circuit for thermal modelling.

D. Temperature model

Thermal effects modelled at cell level using an ECM, as illustrated in Fig. 7. The underlying processes such as heat flow dQ/dt or temperature are converted to current and voltage. Therefore, radiation, convection and heat conduction are represented by a voltage drop over nonlinear thermal heat transfer resistances as:

$$R_{\text{radiation}} = T_1 - T_2/(A \cdot \alpha_{1,2} \cdot (T_1^4 - T_2^4)) \quad (5)$$

$$R_{\text{convection}} = 1/A \cdot \alpha \quad (6)$$

$$R_{\text{conduction}} = d/\lambda \cdot A \quad (7)$$

with d representing the thickness, λ the specific heat conductivity and α the convection coefficient.
The temperature of a volume element is calculated using the current temperature and its change. The temperature of an element is increased by the temperature difference $\triangle T$, once a heat $\triangle Q$ is applied. The heat is proportional to $\triangle T$:

$$\triangle Q = C \cdot \triangle T \quad (8)$$

C represents the heat capacity of the element and depends on the material and mass. $\triangle T$ is calculated by:

$$\frac{dT}{dt} = \frac{1}{C}\left(\frac{dQ_{received}}{dt} - \frac{dQ_{delivered}}{dt}\right) \quad (9)$$

At battery pack level the following heat transfer phenomena are considered:

a. transfer within a cell (mostly heat conduction)
b. transfer to the environment (convection and radiation)
c. transfer to neighbouring cells (heat conduction, similar to a.)

The heat conductivity is defined by:

$$\frac{dT}{dt} = \frac{1}{C} \cdot \sum(-T - T_i/R_i) \quad (10)$$

with index i describing the thermal resistance R_i and conductivity of the neighbours. The heat exchange with the environment is based mainly on the convection and radiation and described as:

$$\frac{dT}{dt} = \frac{1}{C} \cdot \sum\left(\frac{-dQ_{conv}}{dt} - \frac{dQ_{rad}}{dt}\right) \quad (11)$$

with

$$\frac{dQ_{conv}}{dt} = \alpha_{con} \cdot A \cdot (T - T_i) \quad (12)$$

$$\frac{dQ_{rad}}{dt} = \alpha_{con} \cdot A \cdot (T^4 - T_i^4) \quad (13)$$

The thermal parameters were extracted using a non-destructive evaluation of the battery by anisotropic thermal diffusivity measurement by means of thermography. After exciting the front plane of the battery with a flash lamp (in-plane measurement) or induction coil (through-plane measurement) the rise of temperature in the rear face plane is recorded by a thermal imaging camera. The extracted parameters for the Kokam cell are presented in Table I.

TABLE I: Thermal parameters extracted by anisotropic thermal diffusivity measurement

heat conductivity in-plane	33	$W/(m \cdot K)$
heat conductivity through-plane	0.61	$W/(m \cdot K)$
Density	1.982	$kg/(dm^3)$
Heat capacity	860	$J/(kg \cdot K)$
Mass	1.18	kg

E. Aging model for HIL simulation

In order to emulate the variation of cell-to-cell characteristics the impedance-based ECM is coupled to an aging model. This model maps the results of the parameterization from accelerated aging tests of battery cells cycled with a real driving cycle. A physical based function is extracted from the experimental data in order to describe the aging state of the cell. All the cycling tests were carried out at different temperatures based on the average yearly temperatures of Germany. The increase of internal resistant and loss of capacity are monitored every 100 driving cycles conducting checkup or reference performance tests.

The checkup tests consist of a pulse power characterization test for current dependency investigation and

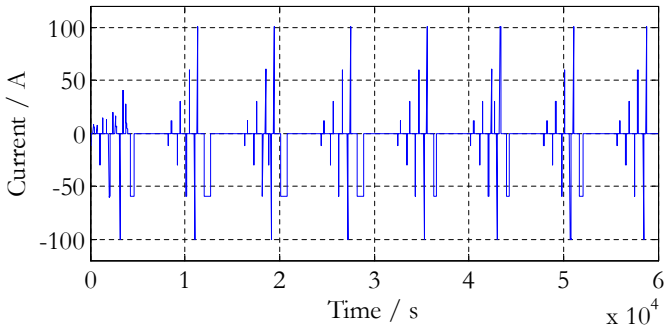

Fig. 8: Pulse power characterization profile.

a capacity check. The pulse power characterization test is intended to determine the internal resistance over the cells usable voltage range using a test profile that includes both discharge and charge/regen pulses. The test profile in Fig. 8 is applied to the cell under test for different temperatures in consecutive steps of 10% SOC. The SOC is adjusted based on the accumulated Ah referring to the nominal capacity. The resistance is calculated as the difference between the voltage before the discharge pulse and Δt after the beginning of the discharge pulse, divided by the amplitude of the current. The capacity check tests consist of a typical CCCV charge and CC discharge cycle conducted at 1 C-rate and different temperatures. It should be noted that during the checkup tests the cells are operated always inside a safe operating area limited by certain temperatures, voltages and currents specified in the manufacturer's data sheet.

Finally, the ZARC element parameters are identified based on EIS measurements. The impedance spectra are also measured at different SOC and temperatures for using frequencies between 10 mHz and 5 kHz.

To represent the individual aging states of the cells, three parts are integrated as shown in Fig.9:

1) Impedance-based electric model
2) Thermal model
3) Aging simulation

Every aging parameter was extracted separately and can be changed offline or on-the-fly while running a HIL simulation. Hence, it is possible to represent realistic operating conditions of multi-cell battery packs by applying a statistical distribution of the individual aging states. Therefore, using the three part model proposed here, a full range of realistic scenarios can be addressed. This means that the functional safety of the system can be verified in an early development stage.

IV. Commercial BMS under test

The commercial BMS under test is the sBMS v6 provided by Lithium Balance A/S. The BMS uses a

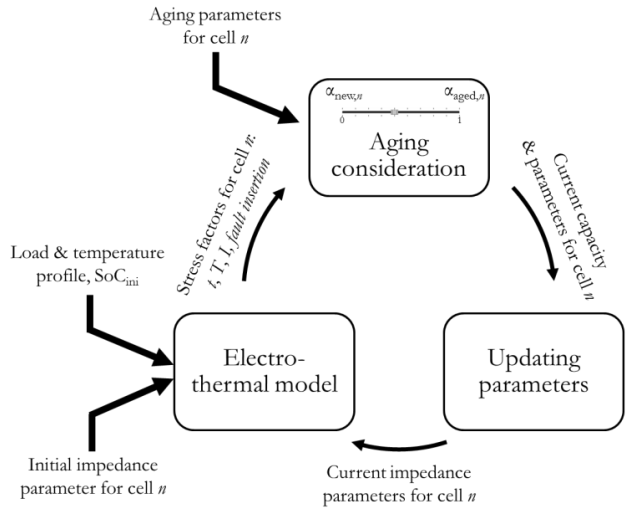

Fig. 9: On-line integration of individual cell aging simulation with electro-thermal model.

master-slave configuration, where each slave unit can be configured to supervise 8 cells and 2 temperatures. The slave is capable of passive balancing with up to 1 A simultaneously on all 8 cells and will automatically reduce the balancing power if the heat cannot be dissipated at high enough rates. A total of 32 slave units can be used for each master, giving a total of 256 supervised cells and 64 temperature inputs. The master is capable of measuring LIB pack current, LIB pack voltage, isolation faults, and contactor faults. Communication to external systems is provided through a configurable CAN bus interface, where any parameter can be broadcasted. The control of contactors, switches and fans are all implemented in the BMS and can have a multitude of configurations.

V. Experimental Results

In this section, the experimental results resulting for HIL tests of the commercial BMS are presented. The testing performed on the HIL setup and the commercial BMS comprises: cell voltage and pack current accuracy, temperature tracking, cell balancing and fault insertion.

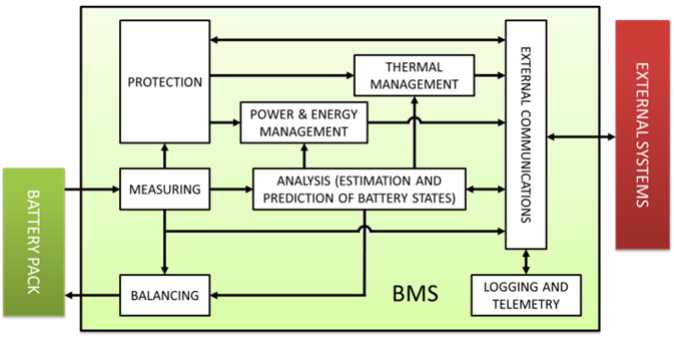

Fig. 10: Overview of typical BMS functions.

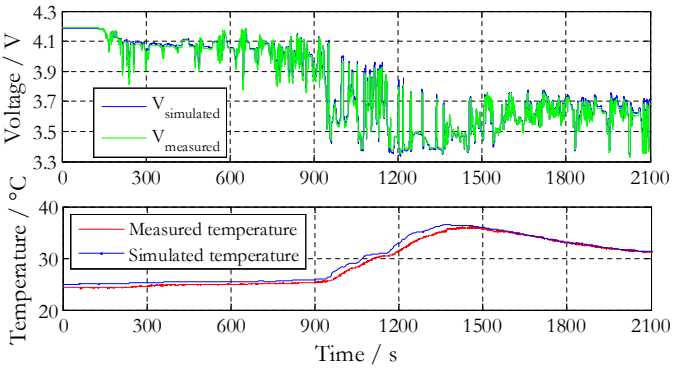

Fig. 11: Electro-thermal battery model validation between measurement data and model simulation.

A. Model Validation

As a first step, the electro-thermal model is validated in simulations. Fig. 11 shows the simulated voltage response in comparison to the real measured voltage. The dynamic load profile applied was logged in a real EV and processed for simulation. It can be noticed that the model is able to follow the measured voltage response. The same can be concluded from the temperature comparison. The starting temperature is initialized at 25°C and stays constant due to lower dynamical driving. As soon as the load current increases, a rise in temperature is observed due to higher power losses. The model is also able to follow this trend accurately. Therefore its applicability for HIL simulation is demonstrated. or State-of-Health (SoH) estimation, can be analyzed in future tests.

B. Validation of BMS with HIL emulation

In the next step, the model-based battery simulation is converted to C-code and emulated in real-time on the HIL test bench. Therefore, communication interfaces between the HIL and the BMS are defined and implemented. Fig. 12 shows the emulated cell voltages for 32 cells connected in series. The entire scenario aims to represent a typical driver behavior, where a standard user drives to work with a fully charged vehicle. After arriving at the workplace the car should not be charged immediately, since higher SOC levels during OCV conditions may accelerate aging. It is assumed that the BMS is able to calculate the charging time and only starts the charging procedure when it is required according to the driver usage patterns. The dynamic characteristics such as initial impedance parameters, initial cell temperature and initial ambient temperature are selected assuming that the underlying distribution is normal. Parameters can be changed off-line or on-the-fly during emulation. An exemplary charging scenario is illustrated in Fig. 13. Different initial voltages and cell-to-cell characteristics are considered at the beginning of charge. These voltage differences are equalized by the BMS balancing circuits during the charging process, in order to maximize usable battery capacity. The parameters for the balancing window are defined in the GUI of the commercial BMS. After the BMS initiates the charging process, the voltage increases gradually ($t = 5500$s). As soon as one cell reaches the cell target voltage, the balancing is activated as illustrated in Fig. 13.
Due to balancing, the overshoot is reduced within the allowable window. All the cells, even though having different characteristics and initial voltages are balanced to the cell target voltage at the end of charge.

C. Fault insertion

When testing a system for its functional requirements, it is important to proof the system for every possible type of fault scenarios and errors. Only a successful pre-testing activity helps to identify potential failure modes events during the battery pack lifetime. Utilizing FMEA at the start of the developing process, which carries out a systematic and structured evaluation, helps to determine the consequences of failure mechanisms. The HIL simulator has to provide all the relevant signals to test and evaluate all safety related functions, including:

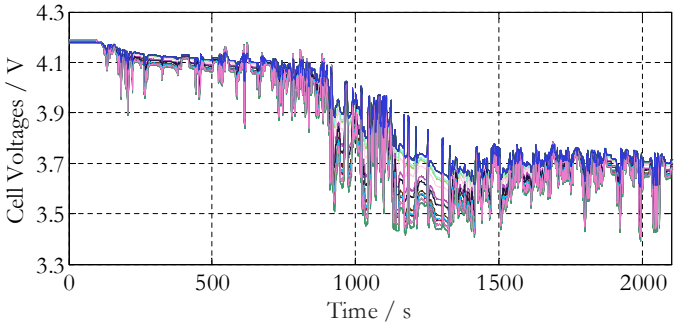

Fig. 12: HIL battery cell emulation using dynamic driving cycle.

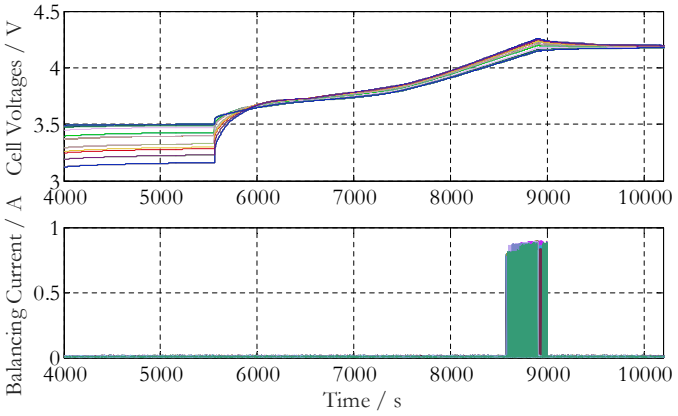

Fig. 13: HIL battery cell emulation during charging.

1) Individual cell and pack voltage
2) Battery current
3) Internal BMS Communication
4) Safety signals (contactor control)
5) Diagnostic signals

Mainly two possible causes for error in the system need to be addressed. First, hardware related errors on the master or slaves of the BMS. Second, cell-based errors like problems in electric connection due to corrosion, intercell-connection or even total failure of the wiring harness.

Fig. 14 illustrates a possible failure caused by a higher internal resistance and self discharge or cell interconnection problems. In order to emulate this fault, additional resistances are added to the cell single model during operation. The figure shows the dynamic response to a load profile recorded in an electrical vehicle.

With the aim of representing realistic operating conditions, a statistical distribution of the individual aging states is applied to the 32 cells in series considered in the setup. At high levels of discharge or charge/regen power, the effects of this cell-to-cell parameter variation are evident.

After a simulation time of 1000 s, the failure mode is applied and within a short time the voltage of cell 1 (blue curve) tends to diverge from the average. Additionally, due to higher resistance in cell 1, the temperature is rising to a higher level in comparison to the healthy cells. Such a scenario has to be detected by the BMS and counter measurements have to be performed, either by BMS or the energy management of the vehicle supervising unit. Complex algorithms computed on a BMS master unit may be able to detect the problem. However, simpler algorithms (e.g. cell voltage average) implemented either at master or slave level may also be able to detect the fault, providing a higher degree of redundancy.

Another possible fault mode considers the interconnection error between the BMS slave board and the terminals of the cell. Vibration, wiring error and blown fuses may lead to a voltage sensor reading of 0 volts.

Then, since the controller is not able to measure the cell voltage, the BMS goes into a critical fault mode. Depending on the configuration settings of the BMS controller, it may not allow to further charge/discharge the pack. This failure mode is simulated by activating a relay while running the HIL emulation. Fig. 15 shows this scenario for a load driving profile with 32 cells in series. After 950 s, the cell voltage of cell 12 (red signal) suddenly drops to zero volts due to fault insertion.

The same kind of test can easily be performed for the temperature sensors, however this fault might not lead to a critical fault mode.

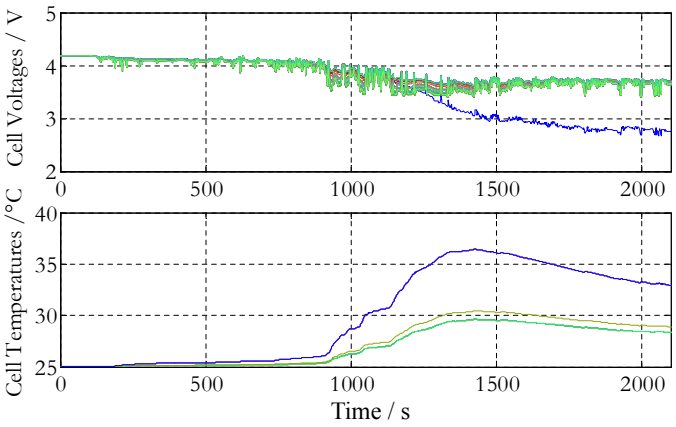

Fig. 14: Model-based fault insertion: Higher series resistance for cell 1.

Since the HIL setup allows for different battery pack topologies, it is also possible to test a multitude of serial, parallel or mixed serial-parallel connections of cells. This is important for testing battery packs consisting of multiple modules and how a BMS handles scenarios related to modules failing or being replaced.

VI. Conclusion

This paper presents a state-of-the-art HIL simulation of a commercial BMS. In comparison with test conducted on real batteries, BMS validation tests conducted on HIL simulators may be more cost and time effective, easier to reproduce and safer beyond the normal range of operation, especially at early stages in the development process or during fault simulation.

The methodology followed in this work comprises following stages: (1) comprehensive review of battery simulation approaches (2) development of an advanced multi-cell impedance-based model (3) development and coupling of an aging model (4) model validation in

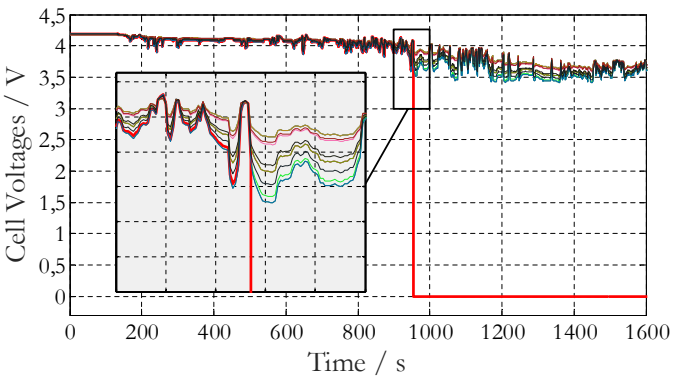

Fig. 15: Model-based fault insertion: Critical zero volt mode.

simulations (5) validation of commercial BMS with HIL emulation (6) fault insertion. For purposes of general functional analysis of a BMS, simple battery models are commonly used in HIL simulation. However, complex models are needed to ensure that all the functionalities of an advanced BMS can be analyzed and validated, e.g. diagnostic algorithms for SOC, SOF or SOH estimation. In this paper, a non-linear dynamic electro-thermal multi-cell ECM coupled with an aging model is presented, taking into account temperature, aging and SOC dependencies. Parameterization is based on experimental data from tests conducted on a commercial 40 Ah high-energy Kokam SLPB100216216H pouch cell. The testing procedures comprised EIS measurements, pulse power characterization tests, capacity checks and anisotropic thermal diffusivity measurements at different aging states. The model is validated in simulations using a dynamic load profile from a real EV. Finally, BMS validation with a HIL simulation is presented. The tests performed on the HIL setup comprised: cell voltage and pack current accuracy, temperature tracking, cell balancing and fault insertion.

Future work will address the following topics: influence of battery models, validation of advanced BMS diagnostic algorithms and a thorough assessment of error and advanced fault insertions.

ACKNOWLEDGMENT

Authors would like to acknowledge The Danish Council for Strategic Research for sponsoring the following projects, the Advanced Lifetime Predictions of Battery Energy Storage (ALPBES) and ReLiable.

REFERENCES

[1] N. Shidore, N. Kim, R. Vijayagopal, D. Lee, A. Rousseau, J. Kwon, B. Honel, and E. Haggard, "Battery in the loop: Battery evaluation in a systems context," in *2014 IEEE Transportation Electrification Conference and Expo (ITEC)*, pp. 1–9, IEEE, 2014.

[2] A. Ebner, F. V. Conte, and F. Pirker, "Rapid Validation of Battery Management System with a Dymola Hardware-in-the-Loop Simulation Energy Storage Test Bench," *The World Electric Vehicle Association Journal*, vol. 1, pp. 205–207, 2007.

[3] H.-S. Song, T.-H. Kim, J.-B. Jeong, B.-H. Kim, D.-H. Shin, B.-H. Lee, and H. Heo, "Verification of battery system model for environmentally friendly vehicles using a battery hardware-in-the-loop simulation," *IET Power Electronics*, vol. 6, pp. 417–424, Feb. 2013.

[4] Y. Yuan, X. Wei, and Z. Sun, *Assessment of power consumption control strategy for battery management system using hardware-in-the-loop simulation*. IEEE, 2008.

[5] S. Kermani, R. Trigui, S. Delprat, B. Jeanneret, and T. M. Guerra, "PHIL Implementation of Energy Management Optimization for a Parallel HEV on a Predefined Route," *Vehicular Technology, IEEE Transactions on*, vol. 60, no. 3, pp. 782–792, 2011.

[6] Y. Xiao-kun, H. Hong-wen, P. Lian-yun, and Z. Xiaolin, "Hardware-in-the-loop simulation on a hybrid power system," in *Power Electronics Systems and Applications (PESA), 2011 4th International Conference on*, pp. 1–5, 2011.

[7] C. Seitl, J. Kathan, G. Lauss, and F. Lehfuss, "Power hardware-in-the-loop implementation and verification of a real time capable battery model," *Industrial Electronics (ISIE), 2014 IEEE 23rd International Symposium on*, pp. 2285–2290, 2014.

[8] T. Mesbahi, N. Rizoug, P. Bartholomeus, and P. Le Moigne, "Li-Ion Battery Emulator for Electric Vehicle Applications," in *Vehicle Power and Propulsion Conference (VPPC), 2013 IEEE*, pp. 1–8, IEEE, 2013.

[9] O. Konig, C. Hametner, G. Prochart, and S. Jakubek, "Battery Emulation for Power-HIL Using Local Model Networks and Robust Impedance Control," *Industrial Electronics, IEEE Transactions on*, vol. 61, no. 2, pp. 943–955, 2014.

[10] A. Thanheiser, W. Meyer, D. Buecherl, and H. Herzog, "Design and investigation of a modular battery simulator system," in *Vehicle Power and Propulsion Conference, 2009. VPPC '09. IEEE*, pp. 1525–1528, IEEE, 2009.

[11] O. Konig, S. Jakubek, and G. Prochart, "Battery impedance emulation for hybrid and electric powertrain testing," in *Vehicle Power and Propulsion Conference (VPPC), 2012 IEEE*, pp. 627–632, IEEE, 2012.

[12] Y. Li, Z. Sun, and J. Wang, "Design for battery management system hardware-in-loop test platform," in *Electronic Measurement & Instruments, 2009. ICEMI '09. 9th International Conference on*, pp. 3–3–402, IEEE, 2009.

[13] G. Pebriyanti, "A lithium-ion battery modeling for a HIL-battery simulator," in *Computer, Control, Informatics and Its Applications, 2013 International Conference on*, pp. 185–190, IEEE, 2013.

[14] L. f. Xu, J. q. Li, J. f. Hua, X. j. Li, and M. g. Ouyang, "Hardware in the loop simulation of vehicle controller unit for fuel cell/battery hybrid bus," in *Vehicle Power and Propulsion Conference, 2009. VPPC '09. IEEE*, pp. 1777–1782, IEEE, 2009.

[15] C. Park, J. Liu, and P. H. Chou, "B#: A Battery Emulator and Power-Profiling Instrument," in *Low Power Electronics and Design, 2003. ISLPED '03. Proceedings of the 2003 International Symposium on*, pp. 288–293, 2003.

[16] A. Florescu, S. Bacha, A. Rumeau, I. Munteanu, and A. I. Bratcu, "PHIL simulation for validating power management strategies in all-electric vehicles," in *Power Electronics and Applications (EPE), 2013 15th European Conference on*, pp. 1–6, IEEE, 2013.

[17] A. Rousseau, S. Halbach, L. Michaels, N. Shidore, N. Kim, N. Kim, D. Karbowski, and M. Kropinski, "Electric Drive Vehicle Development and Evaluation Using System Simulation," in *Proceedings of the 19th IFAC World Congress*, pp. 7886–7891, 2014.

[18] A. Thanheiser, T. P. Kohler, C. Bertram, and H. Herzog, "Battery emulation considering thermal behavior," in *Vehicle Power and Propulsion Conference (VPPC), 2011 IEEE*, pp. 1–5, IEEE, 2011.

[19] T. Baumhofer, W. Waag, and D. U. Sauer, "Specialized battery emulator for automotive electrical systems," in *Vehicle Power and Propulsion Conference (VPPC), 2010 IEEE*, pp. 1–4, IEEE, 2010.

[20] D. Bazargan and S. Filizadeh, "Hardware-in-loop real-time simulation of a battery storage system in a wind generation scheme," in *Electric Power and Energy Conversion Systems*

(EPECS), 2013 3rd International Conference on, pp. 1–6, IEEE, 2013.

[21] D. Kawashima, M. Ihara, T. Shen, and H. Nishi, "Real-time simulation of cooperative demand control method with batteries," in *IECON 2012 - 38th Annual Conference on IEEE Industrial Electronics Society*, pp. 3588–3593, IEEE, 2012.

[22] W. W. Weaver and G. G. Parker, "Real-time Hardware-in-the-Loop simulation for optimal Dc microgrid control development," *Control and Modeling for Power Electronics (), 2014 IEEE 15th Workshop on*, pp. 1–6, 2014.

[23] H. Wu, "Hardware-in-loop verification of battery management system," in *Power Electronics Systems and Applications (PESA), 2011 4th International Conference on*, pp. 1–3, IEEE, 2011.

[24] R. Subramanian, P. Venhovens, and B. P. Keane, "Accelerated design and optimization of battery management systems using HIL simulation and Rapid Control Prototyping," in *Electric Vehicle Conference (IEVC), 2012 IEEE International*, pp. 1–5, IEEE, 2012.

[25] H. Rathmann, C. Weber, W. Benecke, and D. Kahler, "Sophisticated estimation of hardly measurable conditions of lithium-ion batteries," in *Industrial Electronics Society, IECON 2013 - 39th Annual Conference of the IEEE*, pp. 1862–1866, IEEE, 2013.

[26] S. Wu, Y. Zou, X. Peng, and H. Li, "Hardware-in-loop verification of battery management system with RT-LAB," in *Transportation Electrification Asia-Pacific (ITEC Asia-Pacific), 2014 IEEE Conference and Expo*, pp. 1–4, IEEE, 2014.

[27] Q. Wang, X. Z. Wei, and H. F. Dai, "Hardware-in-Loop Test Platform for Electric Vehicle Cell Battery Management System," *Applied Mechanics and Materials*, vol. 29-32, pp. 2398–2403, Aug. 2010.

[28] G. L. Plett, R. Billings, and M. J. Klein, "Desktop and HIL validation of hybrid-electric vehicle battery-management-system algorithms," *SAE 2007 World congress*, 2007.

[29] J. Zeng, J. J. Sun, and Y. Ma, "The System Architecture Design about Test Platform of Battery Management System," *Advanced Materials Research*, vol. 645, pp. 217–220, Jan. 2013.

[30] A. Collet, J. Crebier, and A. Chureau, "Multi-cell battery emulator for advanced battery management system benchmarking," *Industrial Electronics (ISIE), 2011 IEEE International Symposium on*, pp. 1093–1099, 2011.

[31] H. Dai, X. Zhang, X. Wei, Z. Sun, J. Wang, and F. Hu, "Cell-BMS validation with a hardware-in-the-loop simulation of lithium-ion battery cells for electric vehicles," *INTERNATIONAL JOURNAL OF ELECTRICAL POWER AND ENERGY SYSTEMS*, vol. 52, pp. 174–184, Nov. 2013.

[32] W. C. Lee and D. Drury, "Development of a Hardware-in-the-Loop Simulation System for Testing Cell Balancing Circuits," *Power Electronics, IEEE Transactions on*, vol. 28, no. 12, pp. 5949–5959, 2013.

[33] J. V. Barreras, C. Pinto, R. de Castro, E. Schaltz, S. J. Andreasen, and R. E. Araujo, "Multi-Objective Control of Balancing Systems for Li-Ion Battery Packs: A paradigm shift?," in *Proceedings of the IEEE Vehicle Power and Propulsion Conference VPPC*, IEEE Press, 2014.

[34] S. Buller, *Impedance Based Simulation Models for Energy Storage Devices in Advanced Automotive Power Systems*. Aachener Beiträge des ISEA, Shaker Verlag GmbH, 2003.

[35] D. Andre, M. Meiler, K. Steiner, H. Walz, T. Soczka-Guth, and D. U. Sauer, "Characterization of high-power lithium-ion batteries by electrochemical impedance spectroscopy. II: Modelling," *Journal of Power Sources*, vol. 196, pp. 5349–5356, June 2011.

[36] D. Andre, M. Meiler, K. Steiner, C. Wimmer, T. Soczka-Guth, and D. U. Sauer, "Characterization of high-power lithium-ion batteries by electrochemical impedance spectroscopy. I. Experimental investigation," *Journal of Power Sources*, vol. 196, pp. 5334–5341, June 2011.